

# Intermolecular Potentials of the Silane Dimer Calculated with Hartree–Fock Theory, Møller–Plesset Perturbation Theory, and Density Functional Theory

Ching-Cheng Pai, Arvin Huang-Te Li, and Sheng D. Chao\*

*Institute of Applied Mechanics, National Taiwan University, Taipei 106, Taiwan ROC*

*Received: July 7, 2007; In Final Form: September 11, 2007*

We have calculated the intermolecular interaction potentials of the silane dimer at the  $D_{3d}$  conformation using the Hartree–Fock (HF) self-consistent theory, the correlation-corrected second-order Møller–Plesset (MP2) perturbation theory, and the density functional theory (DFT) with 108 functionals chosen from the combinations of 9 exchange and 12 correlation functionals. Single-point coupled cluster [CCSD(T)] calculations have also been carried out to calibrate the correlation effect. The HF calculations yield unbound potentials largely because of the exchange–repulsion interaction. In the MP2 calculations, the basis set effects on the repulsion exponent, the equilibrium bond length, the binding energy, and the asymptotic behavior of the calculated intermolecular potentials have been thoroughly studied. We have employed basis sets from the Slater type orbitals fitted with Gaussian functions (STO- $nG$ ,  $n = 3\sim 6$ ), Pople's medium size basis sets [up to 6-311++G(3df,3pd)], to Dunning's correlation consistent basis sets (cc-pVXZ and aug-cc-pVXZ, X = D, T, Q). With increasing basis size, the repulsion exponent and the equilibrium bond length converge at the 6-31G\*\* basis set and the 6-311++G(3d,3p) basis set, respectively, while a large basis set (aug-cc-pVTZ) is required to converge the binding energy at a chemical accuracy ( $\sim 0.05$  kcal/mol). Up to the largest basis set used, the asymptotic dispersion coefficient has not converged to the expected  $C_6$  value from molecular polarizability calculations. We attribute the slow convergence partly to the inefficacy of using the MP2 calculations with Gaussian type functions to model the asymptotic behavior. Both the basis set superposition error (BSSE) corrected and uncorrected results are presented to emphasize the importance of including such corrections. Only the BSSE corrected results systematically converge to the expected potential curve with increasing basis size. The DFT calculations generate a wide range of interaction patterns, from purely unbound to strongly bound, underestimating or overestimating the binding energy. The binding energies calculated using the OPTXHCTH147, PBEVP86, PBEP86, PW91TPSS, PW91PBE, and PW91PW91 functionals and the equilibrium bond lengths calculated using the MPWHCTH93, TPSSHCTH, PBEVP86, PBEP86, PW91TPSS, PW91PBE, and PW91PW91 functionals are close to the MP2 results using the 6-311++G(3df,3pd) basis set. A correlation between the calculated DFT potentials and the exchange and correlation enhancement factors at the low-density region has been elucidated. The asymptotic behaviors of the DFT potentials are also analyzed.

## I. Introduction

Accurate determination of intermolecular interaction potentials, or van der Waals interactions, is important in the studies of condensed matter physics, materials chemistry, and structural biology. These interactions are crucial in understanding and predicting the thermodynamic properties of molecular liquids and solids,<sup>1</sup> the energy and charge transfers among molecular complexes,<sup>2</sup> and the conformational tertiary structures of macromolecules such as protein and DNA.<sup>3</sup> Intermolecular bonds do not originate from sharing of electrons but rather arise from simultaneous electron correlation of the separated subsystems,<sup>4</sup> and they are relatively soft and nonrigid as compared to intramolecular covalent bonds. Studies of intermolecular interactions abound,<sup>5</sup> but measurements of these interactions are still challenging.<sup>6</sup> The main difficulty in determining intermolecular interactions experimentally resides at limited samplings of the potential energy surface. For example, experiments using the X-ray crystallography or the laser luminescence spectroscopy mainly explore the equilibrium regions of the potential surface,

while thermodynamic measurements in the fluid or solid phase often yield isotropic potential data without the desired stereochemical responses. Moreover, the extracted potentials from experiments sensitively depend on the thermodynamic conditions such as temperature and pressure. Usually, two measurements carried out in different conditions cannot be compared directly but rely on auxiliary theoretical modeling.

It is now well recognized that intermolecular potentials can be calculated in terms of correlation-corrected quantum chemistry methods<sup>7–9</sup> or density functional theory (DFT)<sup>10–11</sup> with improved generalized gradient approximation (GGA) functionals. These calculations are normally done with the supermolecular scheme in which the intermolecular potential is defined as the total energy difference between the supermolecule and the isolated subsystems. In practice, the London dispersion force is the most difficult to calculate because partly of its small magnitude. Because the Hartree–Fock (HF) self-consistent method cannot calculate the dispersion force, an electron correlation-corrected method and a large basis set are required to obtain accurate dispersion forces.<sup>12</sup> Many computational chemistry programs utilize Gaussian type functions to fasten the calculations of Coulomb repulsion integrals. Because

\* To whom correspondence should be addressed. E-mail: sdchao@spring.iam.ntu.edu.tw.

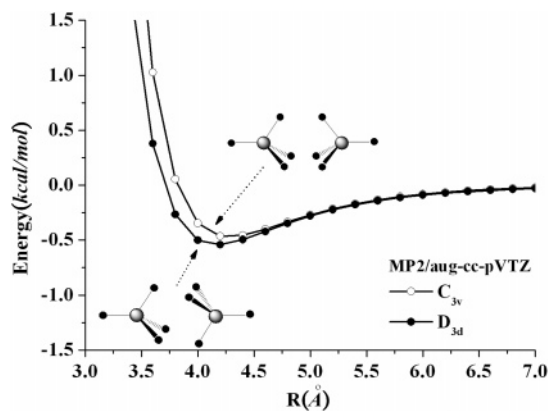


**Figure 1.** The BSSE corrected MP2 potentials using the aug-cc-pVTZ basis set for the  $D_{3d}$  and  $C_{3v}$  conformers of the silane dimer.

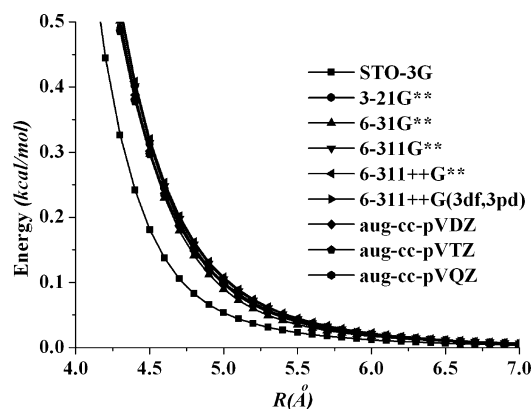


**Figure 2.** The BSSE corrected HF interaction potentials of the silane dimer using several basis sets.

Gaussian type functions are local functions, a large basis set is indispensable to calculate the correlation energy. Moreover, these functions do not have the correct asymptotic behavior of the atomic orbitals. Therefore, the basis set limit of the calculated potential must be estimated so as to be consistent with the conventional perturbation theory based on separated molecules.

Because the dispersion energy is relatively weak, nonpolar atomic and molecular dimers are usually taken as a prototype case to study the dispersion energy. There have been many studies on atomic inert gas dimers which serve as a stepstone to study more complex potential landscapes of molecular dimers.<sup>13</sup> However, there are comparatively fewer studies on molecular dimer systems. Thanks to the extra degrees of freedom and the stereochemical responses, new insights may need to be developed in dealing with molecular dimers. In a previous study,<sup>14</sup> we have thoroughly calculated the interaction potentials of the methane dimer. Methane is a nonpolar molecule with a leading nonvanishing octopole–octopole interaction, and the dominant long-range attraction is thus due to the London dispersion force. Therefore, the study of the methane dimer is a good starting point to investigate the various factors affecting the calculations of the dispersion force, such as the level of the theory, the basis set dependence, and the inclusion of the basis set superposition error (BSSE) corrections. Silane, because of its structural similarity to the methane, is another candidate to perform a prototype study. Besides, silane is a commonly used chemical in semiconductor engineering processes such as the low-pressure vapor-deposited thin-film fabrication process in a microelectromechanical system (MEMS).<sup>49</sup> High-pressure silane crystals could be a good system to demonstrate the insulator–

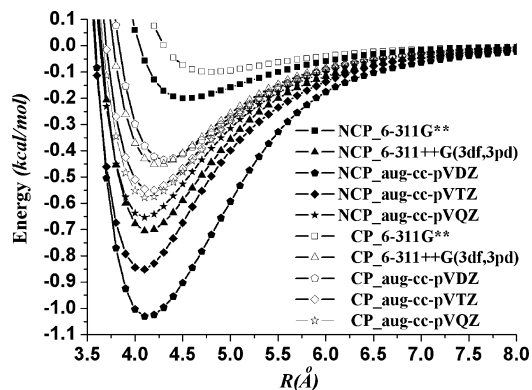


**Figure 3.** The BSSE corrected (CP) and uncorrected (NCP) MP2 potentials of the silane dimer using a series of basis sets.

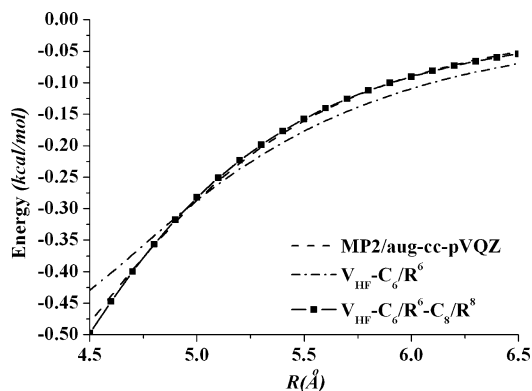


**Figure 4.** Comparison of the BSSE corrected MP2 potential curve calculated at the aug-cc-pVQZ basis set and the sum of the HF potential and the long-range dispersion potentials.

conductor transition in modern solid-state physics.<sup>15</sup> Although the interaction potentials of the methane dimer have been studied extensively, there have been relatively few ab initio studies on the interaction potentials of the structurally similar silane dimer. In fact, it is the case that only very recently a reasonably well-designed quantum chemistry study of the intermolecular interactions of the silane dimer was reported.<sup>16</sup>

In this paper, we perform a comprehensive study on interaction potentials of the prototype silane dimer in terms of the HF, MP2, and DFT methods to gain better understanding of this system. We also perform single-point CCSD(T) calculations for the key structures calculated at the MP2 level of theory to calibrate the correlation effect. The purpose of this paper is to use the state-of-the-art methodology to obtain accurate potential energies for the silane dimer. We would like to study the effect of including the BSSE on the calculated intermolecular interactions. The basis set effects on repulsion exponents, equilibrium bond lengths, binding energies, and asymptotic coefficients of the calculated intermolecular potentials are thoroughly studied. This is achieved using basis sets from STO-3G<sup>17</sup> to aug-cc-pVQZ<sup>19</sup> with the basis number from 26 to 536, respectively. The full potential curves are presented in order to see the overall scope of the potential. In particular, both the BSSE corrected and uncorrected results are presented to emphasize the importance of these corrections. Moreover, in this paper we will assess the utilities of using the available implementation of the density functional theory in determining the intermolecular interactions. From the studies of atomic dimers, it has been found that conventional exchange–correlation functionals based on the local density approximation (LDA) and generalized gradient

**TABLE 1: The Basis Set Dependence of Important Potential Parameters Using the BSSE Corrected HF and MP2 Intermolecular Potentials<sup>d</sup>**

basis set	MP2		HF					MP2				
	number of basis function	CPU time (h)	$A^a$ (kcal/mol)	$\alpha^a$ ( $\text{\AA}^{-1}$ )	$R_0$ ( $\text{\AA}$ )	$R_m$ ( $\text{\AA}$ )	$E_b$ (kcal/mol)	$\omega$ ( $\text{cm}^{-1}$ )	1 term <sup>b</sup>		2 terms <sup>c</sup>	
									$C_6$	$C_6$	$C_8$	
STO-3G	26	1.55	122104.69	2.94	5.98	6.73	-0.001	5.18	317.02	448.94	3203.81	
3-21G	42	1.42	58783.30	2.66	4.75	5.22	-0.037	69.61	1941.38	628.66	54171.60	
6-31G	42	1.49	54009.26	2.64	4.67	5.14	-0.050	87.08	1908.43	660.34	49972.43	
3-21G*	54	1.50	55908.20	2.69	4.55	5.05	-0.058	88.28	2108.34	848.16	49176.41	
6-31G*	54	1.57	53175.77	2.68	4.55	5.04	-0.062	90.25	2062.71	833.95	47916.34	
6-311G*	76	1.56	55354.29	2.67	4.51	5.02	-0.060	81.01	2207.05	930.44	49690.29	
cc-pVDZ	76	2.12	49043.50	2.65	4.17	4.66	-0.166	122.98	3351.38	1728.99	55937.64	
6-31G**	78	1.78	52290.93	2.68	4.45	4.94	-0.077	101.20	2223.41	964.67	47740.30	
6-311G**	100	1.92	53132.34	2.68	4.31	4.80	-0.100	104.08	2685.28	1324.22	49936.37	
6-311++G**	116	2.98	51820.70	2.67	4.29	4.79	-0.105	103.66	2763.58	1297.37	53976.66	
aug-cc-pVDZ	126	4.97	51371.83	2.67	3.83	4.32	-0.435	232.04	5246.08	3221.51	63124.55	
6-311++G(2d,2p)	150	5.41	49711.75	2.67	3.91	4.40	-0.285	180.64	4077.60	2292.74	57950.76	
cc-pVTZ	180	15.86	48247.93	2.66	3.84	4.31	-0.353	212.96	4516.86	2598.04	60292.92	
6-311++G(3d,3p)	184	14.08	49624.69	2.67	3.82	4.30	-0.410	222.38	4869.69	2797.09	65087.98	
6-311++G(2df,2pd)	204	21.20	48903.09	2.67	3.86	4.33	-0.320	208.82	4248.72	2419.41	57507.36	
6-311++G(3df,3pd)	238	43.37	51326.84	2.68	3.77	4.25	-0.454	260.87	5074.31	2956.27	64289.42	
aug-cc-pVTZ	284	137.05	50474.57	2.68	3.70	4.17	-0.551	244.49	5529.30	3291.79	65493.19	
cc-pVQZ	358	232.25	48247.94	2.66	3.72	4.19	-0.489	241.42	5119.50	2688.24	71369.18	
aug-cc-pVQZ	536	1167.03	49979.36	2.68	3.67	4.14	-0.580	293.89	5556.37	3266.28	67621.33	
basis set limit			49317.50	2.68	3.65	4.12	-0.603	378.80				

<sup>a</sup> Fit to the formula  $V_{\text{HF}}(R) = Ae^{-\alpha R}$ . <sup>b</sup> Fit to the formula  $V_{\text{disp}}(R) = -C_6/R^6$ ,  $C_6$  in unit (kcal/mol  $\text{\AA}^6$ ), using data  $R > 4.6 \text{\AA}$ . <sup>c</sup> Fit to the formula  $V_{\text{disp}}(R) = -C_6/R^6 - C_8/R^8$ ,  $C_8$  in unit (kcal/mol  $\text{\AA}^8$ ), using data  $R > 5 \text{\AA}$ . <sup>d</sup>  $R_0$  is the distance at which the potential is zero and  $R_m$  is the equilibrium bond length. The CPU time of the MP2 calculation was recorded on a single node two-processor AMD 250 PC cluster with distributed memory.

**TABLE 2: Comparison of the Binding Energies Using the BSSE Corrected MP2 and CCSD(T) Intermolecular Potentials Calculated at Several Basis Sets<sup>k</sup>**

	Binding Energies					
	cc-pVDZ(76) <sup>a</sup>	cc-pVTZ(180)	cc-pVQZ(358)	aug-cc-pVDZ (126)	aug-cc-pVTZ( 284)	aug-cc-pVQZ (536)
MP2	-0.166	-0.353	-0.489	-0.435	-0.551	-0.580
CCSD(T)	-0.170	-0.378	-0.559	-0.480	-0.632	NA <sup>j</sup>
	Basis Set Limit Estimation					
method	DT <sup>d</sup>	TQ <sup>e</sup>	DTQ <sup>f</sup>	aDT <sup>g</sup>	aTQ <sup>h</sup>	aDTQ <sup>i</sup>
Helgaker et al.	-0.432 <sup>b</sup> (-0.466) <sup>c</sup>	-0.588 (-0.691)	NA	-0.543 (-0.696)	-0.601	NA
Martin	-0.419 (-0.451)	-0.567 (-0.663)	NA	-0.592 (-0.685)	-0.597	NA
numerical	-0.490 (-0.530)	-0.627 (-0.742)	-0.663 (-0.799)	-0.644 (-0.753)	-0.613	-0.603

<sup>a</sup> Number of basis function in parentheses. <sup>b</sup> MP2 basis set limit estimation. <sup>c</sup> CCSD(T) basis set limit estimation in parentheses. <sup>d</sup> Basis set limit estimation with the cc-pVXZ (X = D and T). <sup>e</sup> Basis set limit estimation with the cc-pVXZ (X = T and Q). <sup>f</sup> Basis set limit estimation with the cc-pVXZ (X = D, T, and Q). <sup>g</sup> Basis set limit estimation with the aug-cc-pVXZ (X = D and T). <sup>h</sup> Basis set limit estimation with the aug-cc-pVXZ (X = T and Q). <sup>i</sup> Basis set limit estimation with the aug-cc-pVXZ (X = D, T, and Q). <sup>j</sup> Not available. <sup>k</sup> The basis set limits of the binding energies using the extrapolation methods of Helgaker et al.,<sup>24</sup> Martin,<sup>56</sup> and a numerical method<sup>26</sup> are shown for comparison.

approximation (GGA) cannot calculate the intermolecular interactions to a satisfying level of accuracy.<sup>55</sup> It is thus desirable to investigate to what extent the DFT calculations using available functionals can serve as an alternative for ab initio molecular orbital calculations.

The paper is organized as follows. In section II, we describe the details of these calculations. In section III, the results are presented and discussed. A summary is given in section IV.

## II. Methods and Calculations

Similar to the methane dimer, a large part of the exchange-repulsion interactions of the silane dimer can be calculated by the HF method. The calculation of electron correlation energies depends on the level of the correlation-corrected method, the size of the basis set, and the correction of the BSSE. The state-of-the-art choice of the correlation-corrected method is either the Møller-Plesset (MP $x$ ,  $x = 2-4$ ) perturbation method<sup>20</sup> or the coupled cluster method with iterative single and double

substitutions and with noniterative triple excitations [CCSD(T)] method.<sup>21</sup> Many studies showed that the MP2 results for alkane dimers would not be too much different from those calculated by the much more expensive CCSD(T) method as long as a large basis set has been used.<sup>22</sup> To calibrate the correlation effect, several single-point CCSD(T) calculations for the key structures calculated at the MP2 level of theory have been performed. To study the basis set effects, we have employed comprehensive basis sets from the Slater type orbitals fitted with Gaussian functions (STO- $n$ G,  $n = 3-6$ ),<sup>17</sup> Pople's medium size basis sets [up to 6-311++G(3df, 3pd)],<sup>18</sup> to Dunning's correlation consistent basis sets (aug-cc-pVXZ, X = D, T, Q).<sup>19</sup> The basis set superposition error (BSSE) was corrected by the counterpoise (CP) method of Boys and Bernardi.<sup>23</sup> The MP2 interaction potentials at the basis set limit have been estimated using the methods of Martin,<sup>56</sup> Helgaker et al.,<sup>24</sup> Feller,<sup>25</sup> and a numerical extrapolation scheme on the basis of the Lagrangian formula.<sup>26</sup> The other potential parameters

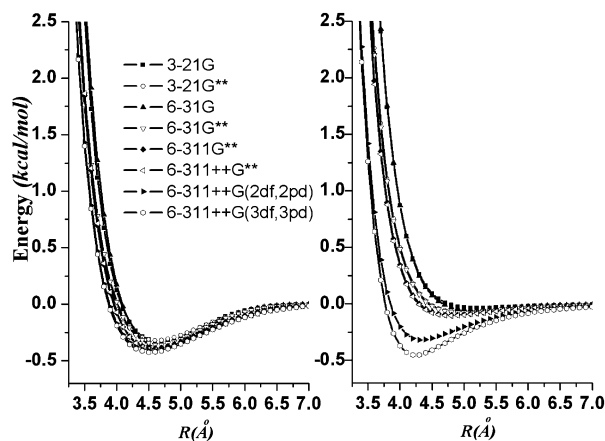


**Figure 5.** The basis set dependence of the DFT potentials calculated with the PW91PW91 functional (left panel). As a reference, the basis set dependence of the MP2 potentials is shown in the right panel.

at the basis set limit are estimated using the numerical extrapolation.

All the HF, MP2, and DFT calculations are performed using the Gaussian 03 program package<sup>27</sup> on a single-node two-processor AMD 250 PC cluster with distributed memory. The equilibrium geometry of a single silane molecule was first optimized at the MP2/6-311++G(3df,3pd) level of theory. Subsequently, the Si–Si distance was sampled in a step of 0.1 Å for a quite large range of intermolecular separation (normally 3–9 Å), resulting in a total of 61 configuration points. During the scan, we allow the individual silane molecule to be fully relaxed. This means that we do not fix the monomer geometry and that the silane molecule is not assumed to be rigid. Although it is not expected to see much deviation from the rigid molecule approximation, inclusion of the intramolecular relaxation could be relevant to molecular dynamics simulations using flexible models.<sup>28</sup>

From a previous energy dissection method,<sup>57</sup> it is found that for a general tetrahedral molecule (such as methane and silane) either the  $D_{3d}$  or the  $C_{3v}$  conformer would be possibly the most stable conformer. We have thus first calculated the potential interaction energies for these two conformers at the MP2/aug-cc-pVTZ level of theory. In Figure 1, we show the comparison of the potential curves for the  $D_{3d}$  and the  $C_{3v}$  conformers. As can be seen, the  $D_{3d}$  conformer is more stable than the  $C_{3v}$  one. Therefore, we will focus on the  $D_{3d}$  conformer in this paper.

### III. Results and Discussions

The intermolecular interaction potentials of the  $D_{3d}$  conformer of the silane dimer have been calculated with the HF, MP2, and DFT methods. We present the results along with discussions and make comparisons among the results.

**A. Hartree–Fock Self-Consistent Field Calculations.** The BSSE corrected HF interaction potentials of the silane dimer using several basis sets are shown in Figure 2. The HF calculations yield purely repulsive potentials without minima for all the basis sets used. This can be attributed to the rather weak electrostatic interaction for the silane dimer. In the short range, the strong exchange–repulsion interaction dominates with little alternation from the electrostatic and induction attractions. The HF potential is insensitive to the basis size as long as the 6-31G\*\* basis set has been used. We can model the HF potential using the repulsive Buckingham function<sup>29</sup>

$$V_{\text{HF}}(R) = Ae^{-\alpha R} \quad (1)$$

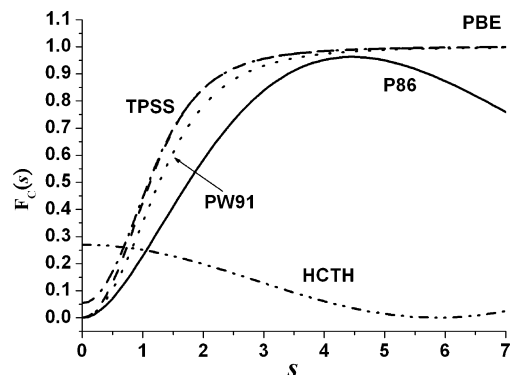


**Figure 6.** The GGA correlation enhancement factor as a function of  $s$  for the TPSS, PBE, PW91, P86, and HCTH correlation functionals. Here,  $r_s = 10$ .

where  $R$  is the Si–Si distance and  $A$  and  $\alpha$  (the repulsion exponent) are the fitting parameters. The dependence of the repulsion exponent on the basis size is shown in Table 1. It is seen that the repulsion exponent converges quickly after the 6-31G\*\* basis set being used.

**B. MP2 Calculations.** Unlike the HF potentials, the MP2 potentials shown in Figure 3 display clear minima and long-range attractive potential tails. Because the contributions from the electrostatic interactions are small, the dispersion energy is mainly responsible for the attractions. The sharp differences between the HF calculations and the MP2 calculations indicate the importance of including the correlation corrections in the wave function calculations. The HF method in principle does not include the correlation effect, so the attraction forces are due exclusively to the correlation effect.

In Figure 3, we compare the MP2 potentials with and without the BSSE corrections (denoted as CP and NCP, respectively). We see very strong dependence of the interaction potentials on the BSSE corrections. The potentials without the BSSE corrections fluctuate with increasing basis size and do not systematically converge to the expected curve at the basis set limit. On the contrary, the BSSE corrected potentials systematically approach the expected curve with increasing basis size. Therefore, the BSSE correction must be considered in calculating the intermolecular interactions, in particular for small basis sets.

The strong basis set dependence and the slow convergence on the dispersion coefficients require an estimation of the important potential features at the basis set limit in a calculated potential. Basis set limit of the binding energy can be approached using Dunning’s basis sets with an extrapolation scheme. We consider three analytical schemes<sup>56,24,25</sup> and a numerical scheme<sup>26</sup> while the results are similar. The binding energies obtained at the basis set limit (using Dunning’s basis sets, aug-cc-pVXZ, X = D, T, Q) are 0.597, 0.601, 0.590, and 0.603 kcal/mol using the methods of Martin,<sup>56</sup> Helgaker et al.,<sup>24</sup> Feller,<sup>25</sup> and the numerical method,<sup>26</sup> respectively. For the other potential parameters, we used the numerical extrapolation on the basis of the vanishing inverse of the number of basis function.<sup>26</sup> These results are shown in Table 1 for comparison.

As shown in Table 1, the basis set effect on the BSSE corrected interaction potentials is significant. The STO-3G basis set yields a very small binding energy. The interaction energy becomes more accurate as one adds polarization functions and augments diffuse functions in the Pople’s basis sets. Small cc-pVDZ and cc-pVTZ basis sets lead to underestimated binding energies and require cc-pVQZ to obtain a result with an accuracy of 0.1 kcal/mol. Augmentation of the diffuse functions has significant effect on optimizing the binding energy. The cc-



**TABLE 3: Comparison of the Bond Lengths (in Å) Calculated with the 108 Exchange–Correlation Functionals Using the 6-311++G(3df,3pd) Basis Set<sup>b</sup>**

exchange functional	correlation functional											
	VWN5	PL	TPSS	PBE	PW91	VWN	VP86	P86	LYP	HCTH93	HCTH	HCTH147
B88	U	U	U	U	U	U	U	U	U	<b>4.41</b>	<b>4.19</b>	<b>4.10</b>
HCTH	6.75	6.75	6.79	6.84	6.84	6.73	7.58	7.58	6.79	6.73	<b>4.51</b>	6.04
OPTX	5.57	5.57	5.64	5.63	5.63	5.52	5.65	5.65	5.52	4.90	<b>4.37</b>	<b>4.56</b>
MPW	5.48	5.48	5.57	5.56	5.55	5.44	5.43	5.42	5.03	<b>4.22</b>	<b>4.12</b>	<b>4.01</b>
TPSS	5.04	5.15	5.03	5.00	4.96	4.95	<b>4.55</b>	<b>4.55</b>	<b>4.63</b>	<b>4.14</b>	<b>4.22</b>	<b>3.96</b>
PBE	4.87	4.87	<b>4.57</b>	<b>4.55</b>	<b>4.51</b>	4.81	<b>4.14</b>	<b>4.14</b>	<b>4.39</b>	<b>4.08</b>	<b>4.06</b>	<b>3.96</b>
PW91	4.81	4.81	<b>4.59</b>	<b>4.57</b>	<b>4.54</b>	4.75	<b>4.14</b>	<b>4.14</b>	<b>4.41</b>	<b>4.07</b>	<b>4.05</b>	<b>3.95</b>
Slater	3.64	3.64	3.30	3.28	3.29	3.61	3.29	3.29	3.44	NA <sup>a</sup>	NA	NA
XAlpha	3.56	3.56	3.24	3.23	3.23	3.53	3.23	3.23	3.38	3.50	3.58	3.44

<sup>a</sup> Not available. <sup>b</sup> As a reference, the MP2 bond length calculated at this basis set is 4.25 Å. The better DFT results of errors within 10% as compared to the MP2 result are marked in black boldface.

**TABLE 4: Comparison of the Binding Energies (in kcal/mol) Calculated with the 108 Exchange–Correlation Functionals Using the 6-311++G(3df,3pd) Basis Set<sup>b</sup>**

exchange functional	correlation functional											
	VWN5	PL	TPSS	PBE	PW91	VWN	VP86	P86	LYP	HCTH93	HCTH	HCTH147
B88	1.342	1.341	1.132	1.111	1.092	1.250	0.821	0.817	0.900	−0.018	−1.994	−0.602
HCTH	−0.004	−0.004	−0.003	−0.003	−0.003	−0.005	−0.001	−0.001	−0.002	−0.002	−0.837	−0.010
OPTX	−0.015	−0.016	−0.015	−0.015	−0.015	−0.027	−0.006	−0.006	−0.025	−0.169	−1.803	<b>−0.443</b>
MPW	−0.063	−0.063	−0.059	−0.060	−0.060	−0.075	−0.045	−0.045	−0.080	−0.756	−2.818	−1.500
TPSS	−0.057	−0.133	−0.066	−0.066	−0.067	−0.078	−0.121	−0.124	−0.175	−0.889	−3.248	−1.625
PBE	−0.129	−0.130	−0.188	−0.191	−0.200	−0.156	<b>−0.492</b>	<b>−0.499</b>	−0.387	−1.391	−3.465	−2.226
PW91	−0.347	−0.349	<b>−0.411</b>	<b>−0.415</b>	<b>−0.424</b>	−0.382	−0.693	−0.700	−0.591	−1.584	−3.659	−2.428
Slater	−1.871	−1.886	−4.865	−5.120	−5.062	−2.070	−5.989	−6.014	−4.035	NA <sup>a</sup>	NA	NA
XAlpha	−2.126	−2.143	−5.403	−5.671	−5.601	−2.344	−6.580	−6.580	−4.484	−5.501	−7.012	−7.100

<sup>a</sup> Not available. <sup>b</sup> As a reference, the MP2 binding energy calculated at this basis set is −0.454 kcal/mol. Positive values represent unbound dimer structures, and the energies are calculated at  $R = 4.25$  Å. The better DFT results of errors within 10% as compared to the MP2 result are marked in black boldface.

pVTZ basis set underestimates the energy by 40%, while the aug-cc-pVTZ basis set underestimates only 9% of the binding energy. Some subtle basis set features can also be observed. For small basis sets, adding polarization functions to the basis set does not significantly change the potential. On the other hand, augmentation of the diffuse functions has a pretty significant effect. For example, the aug-cc-pVDZ energy is very close to the high-level 6-311++G(3df, 3pd) and the cc-pVQZ results. Together with the diffuse functions, adding more polarization functions also improves the accuracy of the calculated potential. For example, the 6-311++G(2d,2p) underestimates the binding energy by 50%, while the 6-311++G-(3df, 3pd) yields a binding energy by 25% lower than the MP2 energy at the basis set limit.

With the wide span of the basis sets used, the basis set dependence of important potential parameters can now be fully studied. In Table 1, we present the BSSE corrected data for the equilibrium bond length, the binding energy, and the asymptotic behavior.  $R_0$  is the distance at which the potential is zero and can be obtained from a two-point interpolation of the calculated data. The bond length  $R_m$ , the binding energy  $E_b$ , and the intermolecular vibration frequency  $\omega$  can be obtained through a harmonic modeling of the three lowest potential data near the equilibrium regions.  $C_6$  and  $C_8$  are the dispersion coefficients and can be obtained through a nonlinear fitting of the long-range potential data. With increasing basis size, the equilibrium bond length converges at the 6-311++G(3d,3p) basis set to a 0.2 Å accuracy, while a pretty large basis set (aug-cc-pVTZ) is required to converge the binding energy at a chemical accuracy ( $\sim 0.05$  kcal/mol). On the other hand, up to the largest basis set used, the asymptotic behavior has not yet converged to the expected  $C_6$  value from the calculated monomer polarizability ( $\sim 4734.47$  kcal/mol Å<sup>6</sup>).<sup>30–32</sup> It is well-known that the long-range interactions can be represented by an infinite series

involving higher order terms  $C_8$ ,  $C_{10}$ , and so forth. Inclusion of the higher order term is important if shorter range data were used for the modeling. For example, as shown in Figure 4, the long-range curve can be reproduced better by including the  $C_8$  term. Similar to our previous study on the methane dimer,<sup>14</sup> we attribute the slow convergence partly to the inefficacy of using the MP2 method with Gaussian functions to calculate long-range interactions. Therefore, the basis set limit of the calculated potential must be estimated so as to be consistent with the conventional perturbation theory. Together with the nonlinear scaling of the computational cost with respect to the basis size, this is actually the main practical reason for the difficulty of obtaining dispersion interactions through ab initio molecular orbital methods. Also, notice that the magnitude of the harmonic vibration frequency ( $\omega \sim 294$  cm<sup>−1</sup> calculated with MP2/aug-cc-pVQZ) indicates that the zero-point energy correction to the binding energy can be significant. This anharmonicity in the intermolecular vibrational motion should be taken into account in analyzing spectra involving van der Waals complexes.<sup>58</sup>

To calibrate the correlation effect, we perform single-point CCSD(T) calculations at several key structures (one at the repulsion region, three at the minimum region, and one at the asymptotic long-range region) using the basis set up to aug-cc-pVTZ. As shown in Table 2, the MP2 results are generally accurate up to 0.1 kcal/mol as compared to those calculated with the CCSD(T) method. The basis set limits of the binding energy have also been obtained using several analytical and numerical extrapolation methods. The results using different extrapolation methods are close to each other within the 0.1 kcal/mol accuracy. The same level of accuracy has also been found before for the methane dimer case.<sup>22</sup>

**C. Density Functional Theory.** We have examined the basis set effect on the DFT potentials in a similar manner as in the HF and MP2 calculations (see Figure 5). We found that in

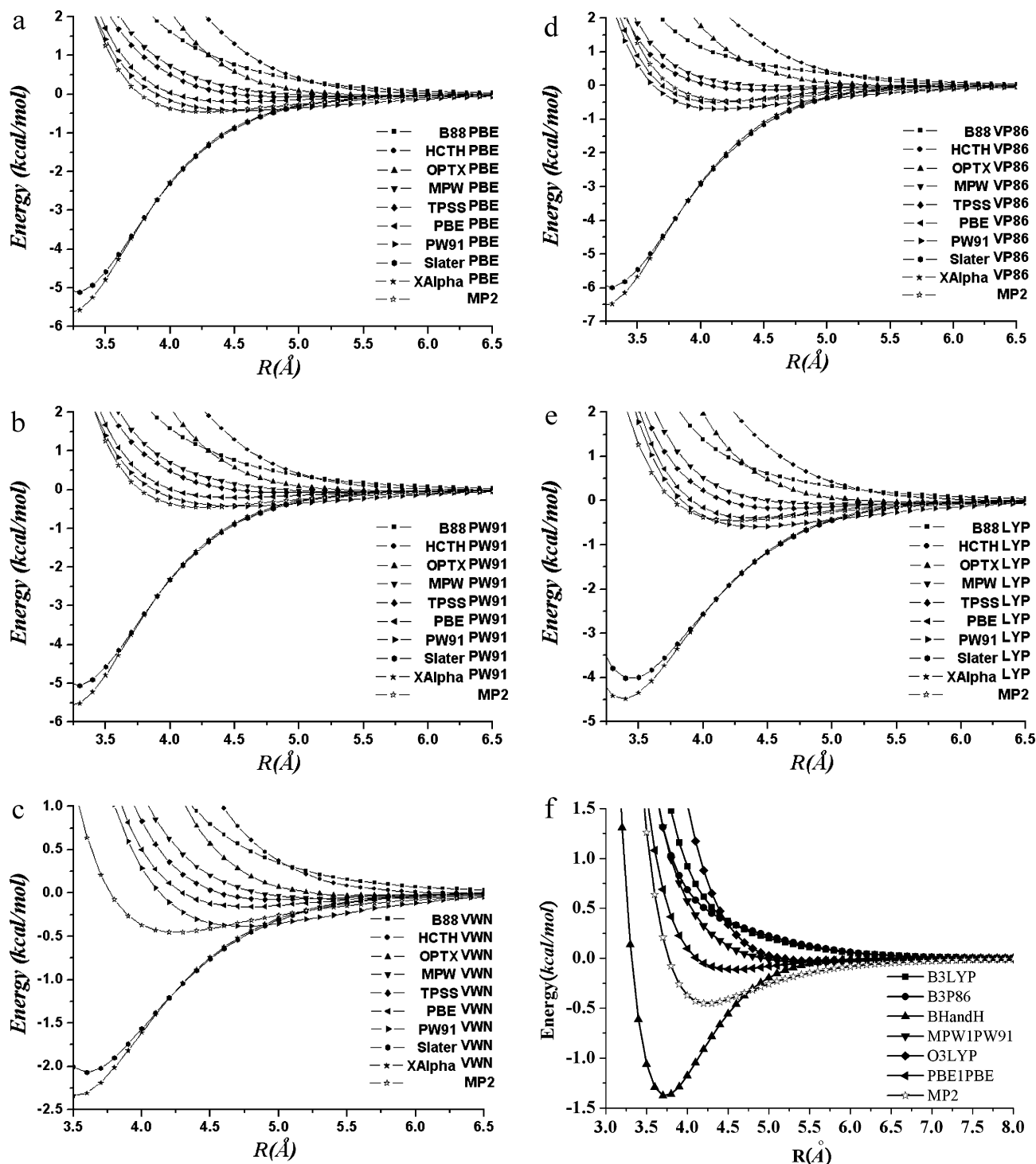


**Figure 7.** The BSSE corrected DFT potential curves with varying exchange functionals by fixing (a) PBE, (b) PW91, (c) VWN, (d) VP86, and (e) LYP correlation functionals. (f) The DFT potentials using several hybrid functionals (B3LYP, B3P86, BHandH, MPW1PW91, O3LYP, and PBE1PBE).<sup>59</sup> The MP2 potential curve is also shown as a reference.

general the DFT potentials converge at a larger basis set than the HF potentials but at a smaller basis set than the MP2 potentials. Therefore, only the 6-311++G(3df,3pd) basis set is used to obtain the DFT potentials which are compared to the MP2 potentials calculated at the same basis set.

The density functionals used in the present work include the 108 combinations chosen among 9 exchange (B88,<sup>33</sup> OPTX,<sup>34</sup> MPW,<sup>35</sup> PBE,<sup>36</sup> PW91,<sup>37</sup> TPSS,<sup>38</sup> Slater,<sup>39</sup> HCTH,<sup>40</sup> and XAlpha<sup>41</sup>) and 12 correlation (TPSS,<sup>38</sup> PBE,<sup>36</sup> PW91,<sup>37</sup> P86,<sup>42</sup> VP86,<sup>42,43</sup> VWN5,<sup>43</sup> PL,<sup>44</sup> VWN,<sup>43</sup> LYP,<sup>45</sup> HCTH93,<sup>46</sup> HCTH,<sup>40</sup> and HCTH147<sup>46</sup>) functionals. We intend to examine the relative

performance of the chosen exchange and correlation functionals in determining the interaction potentials for the silane dimer. The chosen functionals are selective representations of the most commonly used density functionals for van der Waals interactions in current literature. Our previous studies showed that several functionals could yield reasonable binding energies of the methane dimer interaction.<sup>14</sup> In this study, we would like to check the applicability of these functionals for the silane dimer.

In Table 3, we show the bond lengths from the calculated DFT potentials using the 108 exchange–correlation functionals,

displayed as the row and the column items, respectively. Roughly, the bond lengths descend across the row and down the column. Compared with the MP2 result (4.25 Å), we find that the TPSSHCTH and MPWHCTH93 functionals yield a value (4.22 Å) close to the MP2 result. Other candidates are marked in boldface in Table 3. Table 4 presents the calculated binding energies using the 108 exchange–correlation functionals in a particular order. In this order, the (negative) DFT potentials descend across the row and down the column. The results clearly demonstrate the relative performance of the exchange and the correlation functionals in the DFT calculations. By fixing the PW91 as the exchange functional, for example, all correlation functionals yield bound potentials. On the other hand, by fixing the PW91 as the correlation functional, the varying exchange functionals much underestimate or overestimate the binding energy. One of the combinations, OPTXHCTH147, yields a binding energy (−0.443 kcal/mol) close to the MP2 result (−0.454 kcal/mol). Other candidates yielding better results include the PBEVP86, PBEP86, PW91TPSS, PW91PBE, and PW91PW91 functionals. Previous studies on van der Waals systems<sup>47</sup> have shown that the exchange functional plays an essential role in determining the binding energy while the correlation part of a density functional does not significantly affect the DFT calculations. Our results are consistent with the former observation, while we see appreciable effects because of the choice of the correlation functional. It is also found that the calculated binding energies are related to the large reduced density gradient,  $s = |\nabla\rho|/(2(3\pi)^{1/3}\rho^{4/3})$ ,  $\rho$  being the density, of the GGA enhancement factor.<sup>47</sup> However, for dispersion interactions, a large  $s$  actually means a low density because the electron overlapping is relatively small. To further analyze the calculated results, we examine the large  $s$  behavior of the GGA enhancement factors at the low-density region.

The performance of varying the GGA exchange functionals for a fixed correlation functional has been related to the behavior of the GGA enhancement factor  $F_X(s)$  of the exchange functional for the large reduced density gradient region.<sup>47</sup> On the other hand, the performance of varying the GGA correlation functionals for a fixed exchange functional has not been well recognized. For low density and large  $s$ , the contribution of correlation energy becomes significant.<sup>36</sup> In Table 4, we see that for a fixed exchange functional, it may amount to a wide range of binding energies by varying the correlation functional. Because most GGA correlation functionals use the LDA correlation as an additive ingredient in the definition, to clearly show the nonlocal effect, an enhancement factor is defined by

$$F_C(s, r_s) = 1 - \frac{\epsilon_C^{\text{GGA}}}{\epsilon_C^{\text{LDA}}} \quad (2)$$

where  $\epsilon_C^{\text{GGA}}$  and  $\epsilon_C^{\text{LDA}}$  are the correlation potentials for the GGA and the LDA energy functionals, respectively. The correlation enhancement factor depends on  $s$  and  $r_s$ , where  $r_s = (3/4\pi\rho)^{1/3}$  and is the Wigner-Seitz radius. For van der Waals interactions,  $r_s$  falls in the range of 5–20. By fixing  $r_s = 10$ , we plot the enhancement factor  $F_C(s)$  as a function of  $s$  in Figure 6. We see in Figure 6 that the order of the magnitude of  $F_C(s)$  at medium  $s$  is TPSS > PBE > PW91 > P86 > HCTH. Interestingly, this order is essentially the order of the binding energies calculated by the corresponding functionals across the row in Table 4. These observations clearly show that the DFT binding energies are correlated to the exchange and the correlation enhancement factors at the low-density region.

Figure 7a–e presents the calculated DFT potential curves by fixing five correlation functionals and by varying the exchange

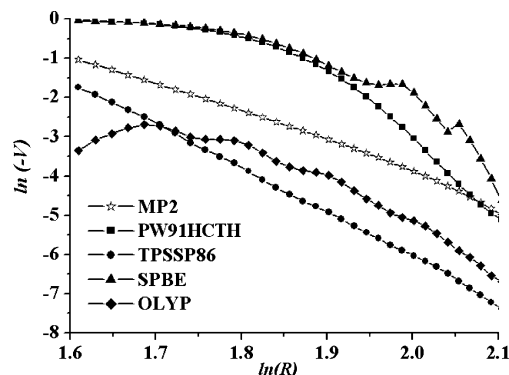


**Figure 8.** The asymptotic behaviors of selective DFT potentials versus the MP2 potential via an analysis of the long-range data.

functions used in this paper. Figure 7f presents the potential curves using several hybrid functionals. We see that the DFT calculations generate a wide range of potential patterns. Some are purely repulsive (such as B88PBE), while others could be overbounded (such as XAlphaVP86). These diverse patterns have been found before and have often been termed “unsystematic”. From our analysis, it is clear that some compensation among the respective exchange and correlation functions must occur to yield a reasonable potential well depth close to the MP2 result. For the silane case, OPTXHCTH147 seems to achieve such appropriate compensation and thus yields a better result. However, exactly which combination should be used for a specific system is unknown a priori. It is hoped that the interesting correlation between the calculated results and the exchange and the correlation enhancement factors shown in Table 4 can provide a useful reference for choosing such a combination.

Finally, we would like to discuss the asymptotic behaviors of some selective DFT potentials and compare them with those obtained from the MP2 reference potential. It is often iterated that a DFT potential cannot be used to model the long-range tail of the van der Waals interaction. However, exactly how bad the situation is for a specific DFT potential has not been systematically studied because partly of insufficient long-range potential data. Figure 8 displays the linear analysis of the potential curves by plotting  $\ln(-V)$  versus  $\ln(R)$ , where  $V$  is the (negative) potential energy by subtracting the HF potential (which is purely repulsive) from the DFT potential and  $R$  is the Si–Si distance. The data for  $R > 5\text{Å}$  have been used to perform this analysis. Notice that the MP2 potential yields a straight line. Generally, the DFT potentials yield erratic long-range behaviors. The deviation from the straight (MP2) line indicates the inefficacy of the DFT potentials. This verifies that DFT potentials calculated using most of the LDA and GGA functionals cannot be used to model the dispersion interactions, in particular, at long-range regions.<sup>48</sup> In this regard, one might resort to other recent approaches to calculate the long-range dispersion interactions.<sup>50–54</sup>

#### IV. Conclusion

In this paper, we have systematically studied the calculated intermolecular potentials of the silane dimer at  $D_{3d}$  conformation using the HF, MP2, and DFT methods. A wide selection of basis sets has been employed to determine the basis set effects on the repulsion exponent, the binding energy, the equilibrium bond length, and the asymptotic behavior of the intermolecular potentials. BSSE corrections are considered as an important factor affecting the quality of the calculated potentials.



From this study and from our previous studies,<sup>14,48</sup> we can draw several useful conclusions about using the current theoretical methods to generate the intermolecular potentials of nonpolar molecular dimers.

(1) The HF calculations yield purely repulsive potentials for nonpolar molecular dimers. This is due to the small electrostatic interactions. The basis size effect of the HF calculations is very small as long as the 6-31G\*\* basis set has been used. The HF method can be used to calculate the exchange–repulsion interactions.

(2) The potential energy minima can be well produced using the MP2 method. The BSSE corrections must be considered to yield systematic results. Basis set effects are significant for many important potential parameters such as bond lengths, binding energies, and dispersion coefficients. Small basis sets, especially without the augmentation of diffuse functions, could produce a severe underestimation of the binding energy and an overestimation of the bond length.

(3) The DFT potentials display a diverse range of patterns of potential curves underestimating or overestimating the binding energy. Some functionals do capture partly the correlation effects. For the silane dimer, the binding energies calculated using the OPTXCHT147, PBEVP86, PBEP86, PW91TPSS, PW91PBE, and PW91PW91 functionals and the equilibrium bond lengths calculated using the MPWHCTH93, TPSSHCTH, PBEVP86, PBEP86, PW91TPSS, PW91PBE, and PW91PW91 functionals are close to the respective MP2 results. The calculated binding energies can be correlated to the asymptotic behaviors of the exchange and the correlation enhancement factors at the low-density region. The long-range DFT potential data cannot be used to model dispersion interaction.

**Acknowledgment.** This work was supported by the National Science Council of Taiwan, ROC (NSC-95-2113-M-002-028-MY3, NSC-95-2120-M-002-006). We acknowledge the National Center for High-performance Computing (NCHC) for providing computing resources.

## References and Notes

- Kaplan, I. G. *Intermolecular Interaction*; Wiley: New York, 2006.
- Charge transfer in DNA: from mechanism to application*; Wagenknecht, H.-A., Ed.; Wiley-VCH: Weinheim, Germany, 2005.
- Hydrogen Bonded Polymers*; Binder, W., Ed.; Springer-Verlag: Berlin, 2007.
- Stone, A. J. *The Theory of Intermolecular Forces*; Oxford University Press: Oxford, U.K., 1996.
- Szalewicz, K.; Patkowski, K.; Jeziorski, B. *Struct. Bond* **2005**, *116*, 43.
- van der Avoird, A.; Wormer, P. E. S.; Moszynski, R. *Chem. Rev.* **1994**, *94*, 1931.
- Rappe, A. K.; Bernstein, E. R. *J. Phys. Chem. A* **2000**, *104*, 6117.
- Chalasiniski, E. R.; Szczesniak, M. M. *Chem. Rev.* **2000**, *100*, 4227.
- Wheatley, R. J.; Tulegenov, A. S.; Bichoutskaia, E. *Int. Rev. Phys. Chem.* **2004**, *23*, 151.
- Zhao, Y.; Truhlar, D. G. *J. Chem. Theory Comput.* **2005**, *1*, 415.
- Grimme, S. *J. Comp. Chem.* **2004**, *25*, 1463.
- Dykstra, C. E.; Frenking, G.; Kim, K. S.; Scuseria, G. E., Eds. *Theory and Applications of Computational Chemistry: The first forty years*; Elsevier: Amsterdam, 2005.
- Ruzsinszky, A.; Perdew, J. P.; Csonka, G. I. *J. Phys. Chem. A* **2005**, *109*, 11015.
- Li, A. H.-T.; Chao, S. D. *J. Chem. Phys.* **2006**, *125*, 094312.
- Pickard, C. J.; Needs, R. J. *Phys. Rev. Lett.* **2006**, *97*, 045504.
- Sakiyama, Y.; Takagi, S.; Matsumoto, Y. *Phys. Fluids* **2004**, *16*, 1620.
- Szabo, A.; Ostlund, N. S. *Modern Quantum Chemistry. Introduction to Advanced Electronic Structure Theory*; Dover: New York, 1996.
- Krishnan, R.; Binkley, J. S.; Seeger, R.; Pople, J. A. *J. Chem. Phys.* **1980**, *72*, 650.
- Dunning, T. H., Jr. *J. Chem. Phys.* **1989**, *90*, 1007.
- Møller, C.; Plesset, M. S. *Phys. Rev.* **1934**, *46*, 618.
- Pople, J. A.; Head-Gordon, M.; Raghavachari, K. *J. Chem. Phys.* **1987**, *87*, 5968.
- Tsuzuki, S.; Honda, K.; Uchimaru, T.; Mikami, M. *J. Chem. Phys.* **2006**, *124*, 114304.
- Boys, S. F.; Bernardi, F. *Mol. Phys.* **1970**, *19*, 553.
- Helgaker, T.; Klopper, W.; Koch, H.; Noga, J. *J. Chem. Phys.* **1997**, *106*, 9639.
- Feller, D. *J. Chem. Phys.* **1992**, *96*, 6104.
- Press, W. H.; Teukolsky, S. A.; Vetterling, W. T.; Flannery, B. P. *Numerical Recipe in C*; Cambridge University Press: Cambridge, U.K., 1996.
- Frisch, M. J.; Trucks, G. W.; Schlegel, H. B.; Scuseria, G. E.; Robb, M. A.; Cheeseman, J. R.; Montgomery, Jr., J. A.; Vreven, T.; Kudin, K. N.; Burant, J. C.; Millam, J. M.; Iyengar, S. S.; Tomasi, J.; Barone, V.; Mennucci, B.; Cossi, M.; Scalmani, G.; Rega, N.; Petersson, G. A.; Nakatsuji, H.; Hada, M.; Ehara, M.; Toyota, K.; Fukuda, R.; Hasegawa, J.; Ishida, M.; Nakajima, T.; Honda, Y.; Kitao, O.; Nakai, H.; Klene, M.; Li, X.; Knox, J. E.; Hratchian, H. P.; Cross, J. B.; Bakken, V.; Adamo, C.; Jaramillo, J.; Gomperts, R.; Stratmann, R. E.; Yazyev, O.; Austin, A. J.; Cammi, R.; Pomelli, C.; Ochterski, J. W.; Ayala, P. Y.; Morokuma, K.; Voth, G. A.; Salvador, P.; Dannenberg, J. J.; Zakrzewski, V. G.; Dapprich, S.; Daniels, A. D.; Strain, M. C.; Farkas, O.; Malick, D. K.; Rabuck, A. D.; Raghavachari, K.; Foresman, J. B.; Ortiz, J. V.; Cui, Q.; Baboul, A. G.; Clifford, S.; Cioslowski, J.; Stefanov, B. B.; Liu, G.; Liashenko, A.; Piskorz, P.; Komaromi, I.; Martin, R. L.; Fox, D. J.; Keith, T.; Al-Laham, M. A.; Peng, C. Y.; Nanayakkara, A.; Challacombe, M.; Gill, P. M. W.; Johnson, B.; Chen, W.; Wong, M. W.; Gonzalez, C.; Pople, J. A. *Gaussian 03, Revision C.02*; Gaussian, Inc.
- Rapaport, D. C. *The Art of Molecular Dynamics Simulation*; Cambridge University Press: New York, 1995.
- Jensen, F. *Introduction to Computational Chemistry*; Wiley: New York, 1999.
- Spackman, M. A. *J. Chem. Phys.* **1991**, *94*, 1295.
- Wu, Q.; Yang, W. *J. Chem. Phys.* **2002**, *116*, 515.
- Becke, A. D.; Johnson, E. R. *J. Chem. Phys.* **2005**, *122*, 154104.
- Becke, A. D. *Phys. Rev. A* **1988**, *38*, 3098.
- Handy, N. C.; Cohen, A. J. *Mol. Phys.* **2001**, *99*, 403.
- Adamo, C.; Barone, V. *J. Chem. Phys.* **1998**, *108*, 664.
- Perdew, J. P.; Burke, K.; Ernzerhof, M. *Phys. Rev. Lett.* **1996**, *77*, 3865.
- Burke, K.; Perdew, J. P.; Wang, Y. In *Electronic Density Functional Theory: Recent Progress and New Directions*; Dobson, J. F., Vignale, G., Das, M. P., Eds.; Plenum: New York, 1998.
- Tao, J.; Perdew, J. P.; Staroverov, V. N.; Scuseria, G. E. *Phys. Rev. Lett.* **2003**, *91*, 146401.
- Kohn, W.; Sham, L. J. *Phys. Rev.* **1965**, *140*, A1133.
- Boese, A. D.; Handy, N. C. *J. Chem. Phys.* **2001**, *114*, 5497; see also the supplemental material EPAPS Document No. E-JCPA6-114-301111.
- Slater, J. C. *Quantum Theory of Molecular and Solids. Vol. 4: The Self-Consistent Field for Molecular and Solids*; McGraw-Hill: New York, 1974.
- Perdew, J. P. *Phys. Rev. B* **1986**, *33*, 8822.
- Vosko, S. H.; Wilk, L.; Nusair, M. *Can. J. Phys.* **1980**, *58*, 1200.
- Perdew, J. P.; Zunger, A. *Phys. Rev. B* **1981**, *23*, 5048.
- Lee, C.; Yang, W.; Parr, R. G. *Phys. Rev. B* **1988**, *37*, 785.
- Boese, A. D.; Doltsinis, N. L.; Handy, N. C.; Sprik, M. *J. Chem. Phys.* **2000**, *112*, 1670.
- Zhang, Y.; Pan, W.; Yang, W. *J. Chem. Phys.* **1997**, *107*, 7921.
- Li, A. H.-T.; Chao, S. D. *Phys. Rev. A* **2006**, *73*, 016701.
- Sakiyama, Y.; Takagi, S.; Matsumoto, Y. *J. Chem. Phys.* **2005**, *122*, 234501.
- Andersson, Y.; Langreth, D. C.; Lundqvist, B. I. *Phys. Rev. Lett.* **1996**, *76*, 102.
- Dobson, J. F.; Dinte, B. P. *Phys. Rev. Lett.* **1996**, *76*, 1780.
- Kohn, W.; Meir, Y.; Makarov, D. E. *Phys. Rev. Lett.* **1998**, *80*, 4153.
- Misquitta, A. J.; Jeziorski, B.; Szalewicz, K. *Phys. Rev. Lett.* **2003**, *91*, 033201.
- Hebelmann, A.; Jansen, G.; Schütz, M. *J. Chem. Phys.* **2005**, *122*, 014103.
- Burke, K.; Perdew, J. P.; Wang, Y. In *Electronic Density Functional Theory: Recent Progress and New Directions*; Dobson, J. F., Vignale, G., Das, M. P., Eds.; Plenum: New York, 1998.
- Martin, J. M. L. *Chem. Phys. Lett.* **1996**, *259*, 669.
- Szczesniak, M. M.; Chalasiniski, G.; Cybulski, S. M.; Scheiner, S. *J. Chem. Phys.* **1990**, *93*, 4243.
- Tao, J.; Perdew, J. P. *J. Chem. Phys.* **2005**, *122*, 114102.
- Gaussian 03 User's Reference and IOps Reference*; Gaussian Inc.: Pittsburgh, PA, 2003.